

APPLICATION OF TIME SERIES ANALYSIS AND STATISTICAL PATTERN RECOGNITION FOR SEISMIC DAMAGE DETECTION

P. Omenzetter¹ and O.R. de Lautour²

Dept. of Civil and Environmental Engineering, The University of Auckland, Auckland, New Zealand

¹Senior Lecturer, Email: p.omenzetter@auckland.ac.nz

²PhD Student, Email: Oliver.deLautour@beca.com

ABSTRACT :

Time series methods are inherently suited to the analysis of regularly sampled Structural Health Monitoring (SHM) data and deserve to be better and more extensively explored. This study focuses on the use of statistical pattern recognition techniques to classify seismic damage based on analysis of the time series model coefficients. Autoregressive (AR) models were used to analyze time histories from a 3-storey laboratory bookshelf structure excited on a shake table and the ASCE Phase II Experimental SHM Benchmark Structure in both healthy and damaged states. The coefficients of these AR models were used as damage sensitive features. Three supervised pattern recognition techniques, Back-propagation Artificial Neural Networks, Nearest Neighbor and Learning Vector Quantization were used to classify damage into states, quantify its severity and determine location. In order to visualize the data and reduce its dimensionality it was compressed using Principal Component Analysis or Sammon mapping. The minimum numbers of sensors required for reliable damage detection were also addressed. The results show that seismic damage can be detected and quantified by the three pattern recognition techniques with a very good accuracy using compressed data and small number of sensors.

KEYWORDS:

Damage Detection, Time Series Analysis, Pattern Recognition, Artificial Neural Networks, Nearest Neighbor, Learning Vector Quantization

1. INTRODUCTION

Time series analysis techniques, originally developed for analysing long sequences of regularly sampled data appear inherently suited to Structural Health Monitoring (SHM). However, their application to SHM can still be considered as emerging and remains relatively unexplored. In a study by Sohn et al. (2000) time series model coefficients were chosen to be damage sensitive features. The authors fitted the dynamic response of a concrete bridge pier using Autoregressive (AR) models. By performing statistical analysis on the AR coefficients, responses coming from several damage states could be distinguished. Omenzetter and Brownjohn (2006) used a vector Seasonal Autoregressive Integrated Moving Average model to detect abrupt changes in strain data collected from the continuous monitoring of a major bridge structure. Gul et al. (2007) presented a study in which AR coefficients from a laboratory steel beam with varying support conditions were classified using a clustering algorithm or multivariate statistics.

In this study, AR models were chosen to fit the acceleration time histories of structures in undamaged and damaged states and the AR coefficients were selected as damage sensitive features. Different data reduction techniques, such as selection of subsets of sensors and AR coefficients, Principal Component Analysis (PCA), and Sammon mapping, were applied to the data for cluster visualization, to ease computational burden, and to discern the most damage sensitive features. The supervised statistical pattern recognition techniques of Back-propagation Artificial Neural Networks (BP ANN), Nearest Neighbour (NN) and Learning Vector Quantisation (LVQ) classification were applied to classify damage into states or locate and quantify damage. The methods were applied to a 3-storey laboratory bookshelf structure and the ASCE Phase II Experimental SHM Benchmark Structure.

2. THEORY

2.1. Autoregressive models

In this study, AR time series models were used to describe the acceleration time histories (Wei 2006). A univariate AR model of order p , or $AR(p)$, for the time series $\{x_t\}$ ($t = 1, 2, \dots, n$) can be written as

$$x_t = \phi_1 x_{t-1} + \phi_2 x_{t-2} + \dots + \phi_p x_{t-p} + a_t \quad (2.1)$$

where $x_t, x_{t-1}, \dots, x_{t-p}$ are the current and previous observations of the series $\{x_t\}$, $\{a_t\}$ is a Gaussian white noise error time series with a zero mean and constant variance, and $\phi_1, \phi_2, \dots, \phi_p$ are the AR coefficients.

2.2. Back-propagation Artificial Neural Networks

Artificial Neural Networks are structures deliberately designed to utilize the organizational principles found in the brain. ANNs are capable of pattern recognition, classification and function approximation. ANNs utilising the supervised error Back-propagation (BP) training algorithm (Rumelhart et al. 1986) are commonly referred to as BP ANNs. A BP ANN consists of interconnected neurons, or basic computational units. These are arranged in several layers: an input layer, hidden layer(s) and output layer. Outputs from a preceding layer become inputs into the following layer. The output y of a single neuron is calculated using the weighted sum of all its inputs as

$$y = f(\mathbf{v}^T \mathbf{x}) \quad (2.2)$$

where \mathbf{x} is the vector of inputs into the neuron, \mathbf{v} is the vector of weights for the neuron, f is the neuron's activation function, and superscript T denotes transposition. The error E at the output layer is a function of the weights for the entire network, denoted by vector \mathbf{w} , and can be written as

$$E(\mathbf{w}) = \frac{1}{2} \mathbf{e}(\mathbf{w})^T \mathbf{e}(\mathbf{w}) \quad (2.3)$$

where $\mathbf{e}(\mathbf{w})$ is an error vector quantifying the difference between the desired outputs and actual outputs. In the training phase, the network calculates the outputs for given inputs and the error is propagated backwards from the output layer to the preceding layers using the back-propagation algorithm. The new weights can be found through the application of the following iterative process:

$$\mathbf{w}_{k+1} = \mathbf{w}_k - \left[\mathbf{J}(\mathbf{w}_k)^T \mathbf{J}(\mathbf{w}_k) + \lambda_k \mathbf{I} \right]^{-1} \mathbf{J}^T(\mathbf{w}_k) \mathbf{e}(\mathbf{w}_k) \quad (2.4)$$

where $\mathbf{J} = \partial \mathbf{e} / \partial \mathbf{w}$ is the error Jacobian matrix, λ_k is the parameter that controls convergence properties, and subscript k denotes the iteration step.

2.3. Nearest Neighbor classification

Nearest Neighbor classification is a simple supervised pattern recognition technique (Kohonen 1997). Given a set of pre-selected and fixed reference or codebook vectors \mathbf{m}_i ($i = 1, 2, \dots, k$) corresponding to known classes, an unknown input vector \mathbf{x} is assigned to the class which the nearest \mathbf{m}_i belongs. Several distance measures can be used including Euclidean and Mahalanobis. The Euclidean distance $D_E(\mathbf{x}, \mathbf{y})$ and Mahalanobis distance $D_M(\mathbf{x}, \mathbf{y})$ between two vectors \mathbf{x} and \mathbf{y} can respectively be calculated using

$$D_E = \sqrt{(\mathbf{x} - \mathbf{y})^T (\mathbf{x} - \mathbf{y})}, \quad D_M = \sqrt{(\mathbf{x} - \mathbf{y})^T \mathbf{\Sigma}^{-1} (\mathbf{x} - \mathbf{y})} \quad (2.5a,b)$$

where $\mathbf{\Sigma}$ is the covariance matrix of a distribution generating vectors \mathbf{x} and \mathbf{y} . The Mahalanobis distance accounts explicitly for the different scales and correlations amongst vector entries and can be more useful in cases in which these are significant.

2.4. Learning Vector Quantization

Learning Vector Quantization is a supervised machine learning technique designed for classification or pattern recognition by defining class borders (Kohonen 1997). Given a set of initial codebook vectors \mathbf{m}_i ($i = 1, 2, \dots, k$) which have been linked to each class region, the input vector \mathbf{x} is firstly assigned to the class which the nearest \mathbf{m}_i belongs, i.e. an NN classification is performed. Subsequent learning is an iterative procedure in which the position of the codebook vectors is adjusted to minimise the number of misclassifications. Let c define the index of the nearest codebook vector, i.e. \mathbf{m}_c . The

$\mathbf{m}_i(t)$ are adjusted according to the following learning rule:

$$\begin{aligned} \mathbf{m}_c(t+1) &= [1 - s(t)\alpha_c(t)]\mathbf{m}_c(t) + s(t)\alpha_c(t)\mathbf{x}(t) \\ \mathbf{m}_i(t+1) &= \mathbf{m}_i(t) \text{ for } i \neq c \end{aligned} \quad (2.6)$$

where t denotes iteration step, $s(t)$ equals +1 or -1 if $\mathbf{x}(t)$ has been respectively classified correctly or incorrectly, and $\alpha_c(t)$ is the variable learning rate for codebook vector \mathbf{m}_c .

2.5. Principal Component Analysis

Principal Component Analysis is a popular multivariate statistical technique often used to reduce multidimensional data sets to lower dimensions (Sharma 1997). Given a set of p -dimensional vectors \mathbf{x}_i ($i = 1, 2, \dots, n$) drawn from a statistical distribution with mean $\bar{\mathbf{x}}$ and covariance matrix Σ , PCA seeks to project the data into a new p -dimensional space with orthogonal coordinates via a linear transformation. Decomposition of the covariance matrix by singular value decomposition leads to

$$\Sigma = \mathbf{V}\Lambda\mathbf{V}^T \quad (2.7)$$

where Λ is a diagonal matrix containing the eigenvalues of Σ ranked in the descending order, and \mathbf{V} is a matrix containing the corresponding eigenvectors or principal components. The transformation of a data point \mathbf{x}_i into principal components is

$$\mathbf{z}_i = \mathbf{V}^T (\mathbf{x}_i - \bar{\mathbf{x}}) \quad (2.8)$$

The new coordinates \mathbf{z}_i are uncorrelated. To reduce the dimensionality, a selection $q < p$ of principal components can be used that retains those components that contribute most to the data variance, thus reducing the dimension of the data to q .

2.6. Sammon mapping

Sammon mapping (Sammon 1969) is a nonlinear transformation used for mapping a high dimensional space to a lower dimensional space in which local geometric relations are approximated. Consider a set of vectors \mathbf{x}_i ($n = 1, 2, \dots, n$) in a p -space and a corresponding set of vectors \mathbf{y}_i in a lower dimensional q -space. The distance between vectors \mathbf{x}_i and \mathbf{x}_j in p -space, D_{ij}^* , and the distance between vectors \mathbf{y}_i and \mathbf{y}_j in q -space, D_{ij} , are respectively given by

$$D_{ij}^* = D(\mathbf{x}_i, \mathbf{x}_j), \quad D_{ij} = D(\mathbf{y}_i, \mathbf{y}_j) \quad (2.9a,b)$$

Mapping is achieved by adjusting the vectors \mathbf{y}_i to minimise the following error function:

$$E = \frac{1}{\sum_{i=1}^n \sum_{j<i}^n D_{ij}^*} \sum_{i=1}^n \sum_{j<i}^n \frac{(D_{ij} - D_{ij}^*)^2}{D_{ij}^*} \quad (2.10)$$

3. APPLICATION TO A 3-STOUREY LABORATORY BOOKSHELF STRUCTURE

3.1. Description of 3-storey laboratory bookshelf structure and experimental program

The 3-storey laboratory bookshelf structure (Figure 1a) used in this study was approximately 2.1m high and constructed from angle aluminum sections and stainless steel. Two angle section thicknesses were used for the columns, either 3.0mm or 4.5mm, for the damaged and undamaged states, respectively. Each column was made of 3×0.7 m high segments in order to make them easily replaceable for simulation of localized damage. The whole structure was mounted on a shake table. The structure was instrumented with four uniaxial accelerometers, one for measuring the table acceleration and one for each story. Accelerations were measured in the direction of ground motion at 400Hz. Afterwards the data was decimated by a factor of eight for time series modeling.

Damage was introduced into the structure by replacing the original 4.5mm thick columns of a particular storey with

3.0mm angles. Four damage states were considered; these were labeled D0, D1, D2 and D3 corresponding to no damage (healthy structure), 1st storey damage, 2nd storey damage and simultaneous 1st and 2nd storey damage. Figure 1b shows the remaining stiffness obtained via model updating for each damage state. Eight scaled earthquake records were used to excite the structure. The earthquakes were scaled so that a range of response amplitudes was obtained. The acceleration time history for each storey was modeled using a separate univariate AR(24) model. The AR coefficients were estimated from a 500-point window advancing 100 points. A data set of 388 points (vectors of AR coefficients) containing 97 points for each damage state was obtained.

As a preliminary investigation to check and visualise the presence of clusters in the data Sammon mapping was used to create a 2D projection of the AR coefficient vectors (Figure 2). It showed some organisation of the data into overlapping bands, although no distinct clusters could easily be drawn. These preliminary insights indicated that higher dimensional data was needed to separate the AR coefficients from the different damage states. To achieve this for multidimensional data simple visual techniques were inadequate and more advanced approaches, such as those discussed next were needed.

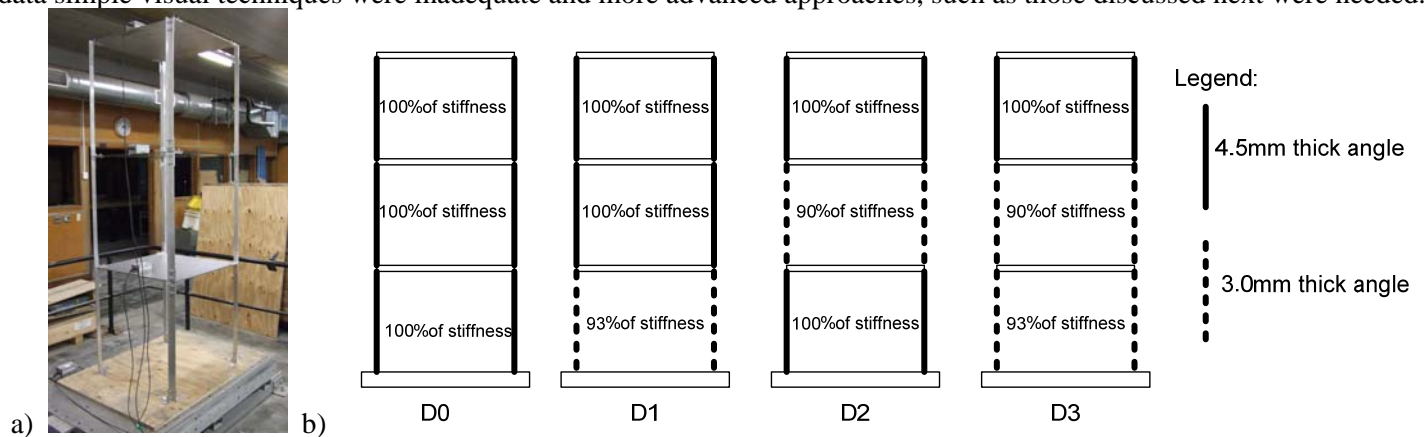


Figure 1. 3-storey laboratory bookshelf structure: a) general view, and b) damage states and remaining stiffness.

3.2. Application of BP ANN to 3-storey laboratory bookshelf structure

Initially, a BP ANN was trained to distinguish between the four damage states only. The damage states D0, D1, D2 and D3 were assigned the vector outputs $[1\ 0\ 0\ 0]^T$, $[0\ 1\ 0\ 0]^T$, $[0\ 0\ 1\ 0]^T$ and $[0\ 0\ 0\ 1]^T$, respectively. A single hidden layer BP ANN with 4 hidden layer neurons was found to give good classifications with only 3 misclassifications or 3%.

Rather than simply classifying damage into several classes, a more useful approach would give information about the extent and location of damage. A BP ANN was subsequently trained to relate the AR coefficients to the remaining stiffness at each storey. A single hidden layer BP ANN with 5 hidden layer neurons was found to give good predictions. The results have been shown in Table 3.1, where the means of the identified remaining stiffness values together with two standard deviation bounds are given. These results show good agreement with the actual stiffness obtained by modal updating. At a 95% confidence level the detected mean values do not differ from the actual values by more than 3.2%. These results show that the ANN has correctly quantified the damage at each story with only a small amount of scatter about the actual remaining stiffness.

3.3. Application of NN classification to 3-storey laboratory bookshelf structure

The previously described NN classification technique was used to classify damage into the states D0-D3. The feature dimension was reduced by projecting the AR coefficients onto the first 60, 40, 30, 20 or 10 principal components using PCA. The 388-point data set was randomly divided into 300 codebook vectors and 88 testing points, respectively. Five different random sets of codebook vectors were considered. Averaging the results from five runs, the obtained number of misclassifications and percentage errors are given in Table 3.2. The Mahalanobis distance out performed the Euclidean by a considerable margin and adequate results with 6% misclassifications were obtained using 20 principal components. Good results, 5% or less misclassifications, were achieved using more than 30 principal components while excellent classification, 1% or less misclassifications, needed 60 principal components. The Euclidean distance, on the other hand,

Table 3.1. ANN identified damage as a percentage of remaining stiffness in 3-storey laboratory bookshelf structure.

Storey	Identified percentage of remaining stiffness (%)			
	D0	D1	D2	D3
1 st	0.996±0.023	0.927±0.027	1.001±0.026	0.935±0.022
2 nd	0.995±0.023	0.997±0.021	0.903±0.029	0.903±0.026
3 rd	1.000±0.000	1.000±0.000	1.000±0.000	1.000±0.000

Table 3.2. Number and percentage of misclassifications using NN classification for 3-storey bookshelf structure.

Number of principal components	Euclidean	Mahalanobis
60	31 (35%)	1 (1%)
40	34 (39%)	3 (3%)
30	30 (34%)	4 (5%)
20	34 (39%)	5 (6%)
10	34 (39%)	10 (11%)

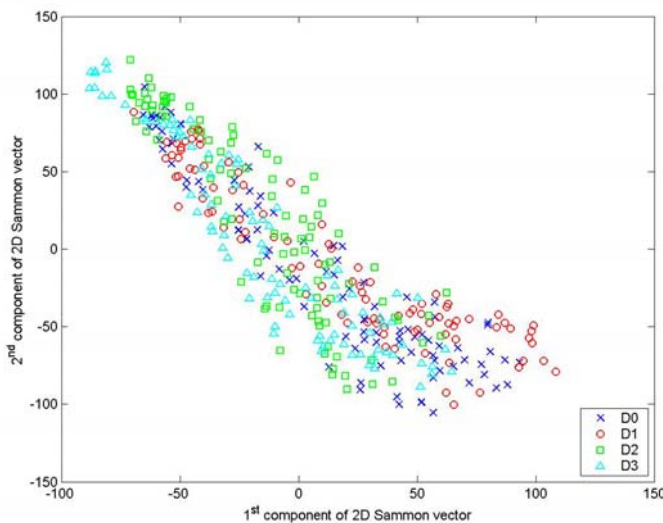


Table 3.3. Number and percentage of misclassifications using LVQ for 3-storey laboratory bookshelf structure.

No. of principal components	Number of codebook vectors		
	30	50	100
30	0 (0%)	0 (0%)	0 (0%)
20	4 (5%)	3 (3%)	3 (3%)
10	17 (19%)	15 (17%)	14 (16%)

Figure 2. Projection of 3-storey laboratory bookshelf structure data via Sammon mapping.

always produced between 35-39% misclassifications. The difference in performance between the Mahalanobis and Euclidean distance measures could be explained by the fact that the Mahalanobis distance accounts for the different scales of each principal component.

3.4. Application of LVQ classification to 3-storey laboratory bookshelf structure

Although NN classification performed well, performance could be improved by using a more advanced classification technique such as LVQ. The LVQ classification was used with the Mahalanobis distance measure and the PCA data reduction technique. The numbers of principal components used were either 30, 20 or 10. The 388-point data set was divided into 300 points for training and 88 points for testing. The number of codebook vectors was chosen to be 30, 50 or 100. These were initialised by random selection from the training data set. The results averaged from five runs with different initialised codebook vectors are shown in Table 3.3. Good classifications were obtained when 20 or more principal components were used while excellent classification was achieved using 30 principal components. Overall, LVQ performed better than NN classification with excellent classifications obtained using 30 principal components.

4. APPLICATION TO ASCE PHASE II EXPERIMENTAL SHM BENCHMARK STRUCTURE

4.1. Description of ASCE Phase II Experimental SHM Benchmark structure and experimental program

The ASCE Phase II Experimental SHM Benchmark Structure is a 4-storey 2-bay by 2-bay steel frame with a 2.5m × 2.5m floor plan and a height of 3.6m, see Figure 3. A full description can be found at the benchmark problem website (ASCE Structural Health Monitoring Committee). The beams and columns are bolted together and bracing is added in all bays.

Four 1000kg floor slabs were placed on the 1st, 2nd and 3rd floors, one per bay. On the 4th floor, four 750kg slabs were used. Two of the slabs per floor were placed off-centre to increase the coupling between translational and torsional motion. A total of 9 damage scenarios were simulated on the structure; these are described in Table 4.1 (the locations in the structure are referred to using their respective geographical directions of North (N), South (S), East (E) and West (W)).



Table 4.1. Damage configurations for ASCE structure.

Config	Damage
1	No damage
2	No bracing on the E side
3	No bracing on floors 1-4 on a bay on the SE corner
4	No bracing on floors 1 and 4 on a bay on the SE corner
5	No bracing on floors 1 on a bay on the SE corner
6	No bracing on E face and floor 2 on N face
7	No bracing in the entire structure
8	Conf. 7 + loosened bolts on fl. 1-4 on E face N bay
9	Conf. 7 + loosened bolts on fl. 1 and 2 on E face N bay

Figure 3. ASCE Phase II Experimental SHM Benchmark Structure.

Of interest in this study were the forced random vibration tests conducted using an electro-dynamic shaker mounted on the SW bay of the 4th floor on the diagonal. Input into the shaker was band-limited 5-50Hz white noise. The structure was instrumented with 15 accelerometers: 3 accelerometers each for the base, 1st, 2nd, 3rd and 4th floors. These measured motion in the N-S and E-W direction. Acceleration data was recorded at 200Hz using a data acquisition system and filtered with anti-aliasing filters. In this research, univariate AR(30) models were fitted to the acceleration data from each accelerometer using the least squares method from 1000-point segments advancing 200 points. A 1035-point data set, consisting of 115 points for each damage configuration, was obtained.

Preliminary investigations showed that projection of the data using Sammon mapping allowed distinct clustering in the data to be seen, see Figure 4. Six large-scale clusters could be seen. Two of the clusters consisted of configurations 1, 5, and 6 and configurations 3 and 4, while the remaining clusters were solely formed by a single configuration. This projection could be used for visual classification of the data once the damage clusters were clearly defined.

4.2. Application of BP ANN to ASCE Phase II Experimental SHM Benchmark Structure

The data from the ASCE Phase II Experimental SHM Benchmark Structure served a twofold purpose. Firstly, it was used to validate the performance of the proposed methods on a more realistic and complex structure with complex damage scenarios. Secondly, the problem of data reduction for multi-sensor SHM systems proved to be of importance and was addressed. Because quantitative information about the damage severity was not readily available, in this application damage classification into the 9 states was attempted. The 9 damage configurations were assigned vector outputs from $[1\ 0\ 0\ 0\ 0\ 0\ 0\ 0\ 0]^T$ to $[0\ 0\ 0\ 0\ 0\ 0\ 0\ 0\ 1]^T$ for configurations 1 to 9, respectively.

A data set of 1035 points was obtained, 115 points from each configuration, and randomly divided into 700 for training and 335 for testing. Using AR(30) models and all 15 accelerometers gave a large ANN input dimension of 450 and training proved to be difficult. Two data reduction techniques were investigated: (i) selection of a subset of AR coefficients and/or accelerometers and (ii) projection of the data using PCA. Several combinations of reduced AR coefficients and accelerometers were investigated to ascertain their practical minimum numbers. The number of AR coefficients was reduced by selecting a few coefficients only as follows: (i) the 1st coefficient, (ii) the 1st 2, (iii) 3, (iv) 4, or (v) 6 coefficients. The number of accelerometers and their location was either (i) the full set (15 accelerometers), (ii) omitted base accelerometers and those on the W face measuring N-S motion (8 accelerometers), or (iii) same as case (ii) but with all accelerometers on stories 1 and 3 omitted (4 accelerometers). A single hidden layer ANN with 5 hidden layer neurons was used for damage classification. Figure 5 shows the number of misclassifications out of the 335-point test data set for the different combinations of reduced AR coefficients and accelerometers. A clear boundary can be seen where performance rapidly deteriorates below the 5% misclassification threshold. The full suite of 15 accelerometers achieved good performance with only 1 AR coefficient, while 2 or 3 AR coefficients were required for 8 or 4 accelerometers,

respectively. For excellent results with less than 1% errors at least 2 or 3 AR coefficients were necessary for 15 and 8 accelerometers, respectively. An overall conclusion that can be drawn from this simulation is that small numbers of AR coefficients and sensors suffice for precise damage classification.

A more methodical approach to dimensionality reduction would retain data of statistical significance only. PCA was used to project the data onto the first 30, 20, 10, or 5 principal components. Using a single hidden layer ANN with 5 hidden layer neurons, the number of classifications with percentage errors for each case is given in Table 4.2. Good damage classification could be achieved by using the first 10 or more principal components and excellent results when using more than 20. Some improvements over the selection of a subset of AR coefficient results were observed especially for small feature dimension. In Figure 5, using 4 accelerometers and 3 AR coefficients (feature dimension of 12) 10 misclassifications are shown. When using 10 principal components, 5 misclassifications were recorded. This demonstrates a superior performance of the more systematic feature reduction approach using PCA over.

4.3. Application of NN classification to ASCE Phase II SHM Experimental Benchmark Structure

The feature dimension of 450 was reduced by projecting the AR coefficients onto the first 20, 10, 5 and 3 principal components using PCA. The 1035-point data set was randomly divided into 700 codebook vectors and 335 testing points. Using NN classification the number of misclassifications and percentage errors are given in Table 4.3. In this case, similar performance was obtained using both distance measures. Excellent performance was obtained using 10 principal components or more. These results show a significant reduction in dimensionality was achievable whilst maintaining good accuracy.

4.4. Application of LVQ classification to ASCE Phase II SHM Experimental Benchmark Structure

Learning Vector Quantization classification was applied to PCA reduced data with the same number of components as above. The same sized training and testing data sets were used. The results from NN classification showed that performance was similar for both distance measures, hence only the Euclidean distance was chosen for LVQ. The number of codebook vectors was chosen to be either 50, 100 or 200. These were initialised by random selection from the training set. The results are shown in Table 4.4. Good or excellent performance was obtained using 20 principal components for all numbers of codebook vectors. Good classification was still achieved using 10 principal components, however, errors became significant once fewer than 5 components were used. Overall, performance was similar to NN classification.

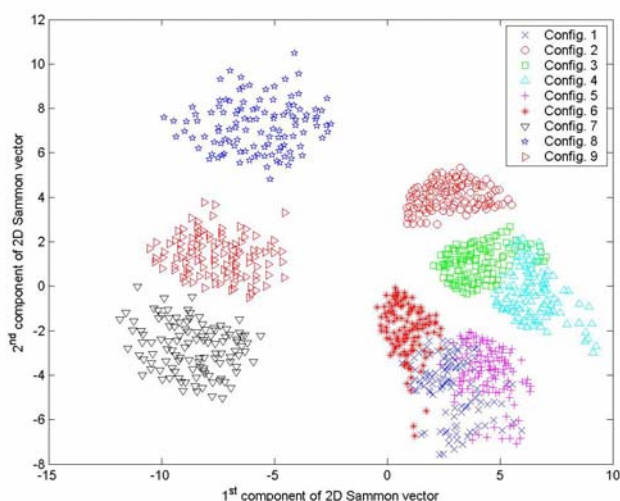


Figure 4. Projection of ASCE Phase II Experimental SHM Benchmark Structure data via Sammon mapping.

5. CONCLUSIONS

AR models were fitted to the acceleration time histories of a 3-storey laboratory bookshelf and ASCE Phase II Experimental SHM Benchmark Structure in undamaged and several damaged states. Clustering of the AR coefficients

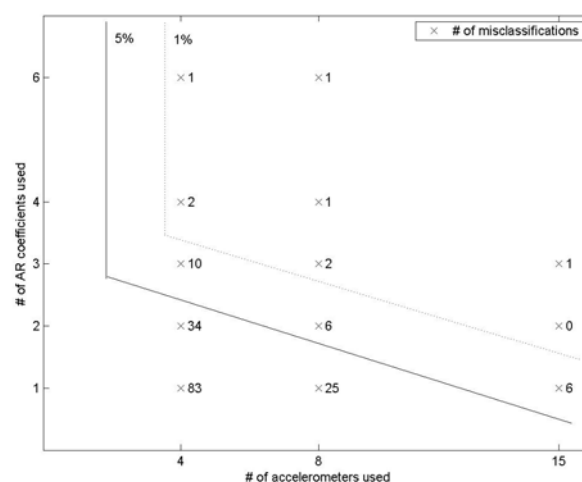


Figure 5. Number of misclassifications produced by BP ANN for ASCE Structure using subsets of AR coefficients and accelerometers.

Table 4.2. Number of misclassifications produced by BP ANN using PCA reduced data from ASCE Structure.

Number of principal components	Number of misclassifications
30	0 (0%)
20	0 (0%)
10	5 (1%)
5	70 (21%)

Table 4.3. Number and percentage of misclassifications using NN classification for ASCE Structure.

Number of principal components	Euclidean	Mahalanobis
20	1 (0.3%)	1 (0.3%)
10	5 (1%)	5 (1%)
5	23 (7%)	24 (7%)
3	62 (19%)	65 (19%)

Table 4.4. Number and percentage of misclassifications using LVQ classification for ASCE Structure.

Number of principal components	Number of codebook vectors		
	50	100	200
20	6 (2%)	5 (1%)	4 (1%)
10	13 (4%)	10 (3%)	6 (2%)
5	24 (7%)	29 (9%)	23 (7%)
3	75 (22%)	68 (20%)	67 (20%)

was investigated using Sammon mapping and distinct clusters corresponding to specific damage states could be seen for the ASCE Phase II Experimental SHM Benchmark Structure. Classification of AR coefficients corresponding to different damage states was performed using BP ANN, NN and LVQ classification on features reduced using PCA. These techniques proved to be effective for classification of damage into states. Overall, the performance of BP ANN, NN and LVQ classification was comparable. Damage in the 3-storey laboratory structure was 97% correctly classified by the BP ANN. NN and LVQ classified 99% and 100% of the data correctly, respectively. For the ASCE Phase II Experimental SHM Benchmark Structure, using 20 principal components 0%, 0.3% and 1% misclassifications were obtained by BP ANNs, NN and LVQ classification, respectively. A study on using subsets of AR coefficients and accelerometers revealed that PCA reduction was a more efficient approach. In addition, BP ANN efficiently detected damage location and accurately estimated its severity in the 3-storey structure with small errors not exceeding 3.2% of the actual values at 95% confidence levels.

ACKNOWLEDGEMENT

The authors would like to express their gratitude for the Earthquake Commission Research Foundation of New Zealand for their financial support of this research (Project No. UNI/535).

REFERENCES

- ASCE Structural Health Monitoring Committee. <http://cive.seas.wustl.edu/wusceel/asce.shm/>.
- Gul, M., Catbas, F.N. and Georgiopoulos, M. (2007). Application of pattern recognition techniques to identify structural change in a laboratory specimen. *Sensors and Smart Structures Technologies for Civil, Mechanical and Aerospace Systems 2007*, San Diego, CA, SPIE.
- Kohonen, T. (1997). *Self-organizing maps*, Springer, Berlin.
- Omenzetter, P. and Brownjohn, J.M.W. (2006). Application of time series analysis for bridge monitoring. *Smart Materials and Structures* **15:1**, 129-138.
- Rumelhart, D.E., Hinton, G.E. and Williams, R.J. (1986). Learning internal representations by error propagation. *Parallel distributed processing: Explorations in the microstructures of cognition*. D. E. Rumelhart and J. L. McClelland, Eds. Cambridge, Massachusetts, MIT Press. 1: 318-362.
- Sammon, J.J.W. (1969). Nonlinear mapping for data structure analysis. *IEEE Transactions on Computers* **C-18:5**, 401-409.
- Sharma, S. (1997). *Applied multivariate techniques*, Wiley, New York.
- Sohn, H., Czarnecki, J.A. and Farrar, C.R. (2000). Structural health monitoring using statistical process control. *Journal of Structural Engineering* **126:11**, 1356-1363.
- Wei, W.W.S. (2006). *Time series analysis: Univariate and multivariate methods*, Pearson, Boston.